applied sciences

MDPI

Article

The Formation Mechanisms of Ultra-Deep Effective Clastic Reservoir and Oil and Gas Exploration Prospects

Yukai Qi [1,2,*], Zongquan Hu [1,2], Jingyi Wang [1,2], Fushun Zhang [1,2], Xinnan Wang [3], Hanwen Hu [1,2], Qichao Wang [1,2] and Hanzhou Wang [1,2]

[1] Petroleum Exploration & Production Research Institute, China Petroleum & Chemical Corporation (SINOPEC), Beijing 100083, China; huzongquan.syky@sinopec.com (Z.H.); wangjingyi.syky@sinopec.com (J.W.); zhangfs.syky@sinopec.com (F.Z.); huhanwen.syky@sinopec.com (H.H.); wangqc.syky@sinopec.com (Q.W.); wanghanzhou.syky@sinopec.com (H.W.)
[2] Key Laboratory of Geology and Resources in Deep Strata, Beijing 102206, China
[3] The Third Oil Production Plant of Daqing Oilfield Limited Company, Daqing 163000, China; xn-wang01@petrochina.com.cn
* Correspondence: qiyk.syky@sinopec.com

Abstract

This study systematically analyzes reservoir formation mechanisms under deep burial conditions, integrating macroscopic observations from representative ultra-deep clastic reservoirs in four major sedimentary basins in central and western China. Developing effective clastic reservoirs in ultra-deep strata (6000–8000 m) remains a critical yet debated topic in petroleum geology. Recent advances in exploration techniques and geological understanding have challenged conventional views, confirming the presence of viable clastic reservoirs at such depths. Findings reveal that reservoir quality in ultra-deep strata is preserved and enhanced through the interplay of sedimentary, diagenetic, and tectonic processes. Key controlling factors include (1) high-energy depositional environments promoting primary porosity development, (2) proximity to hydrocarbon source rocks enabling multi-phase hydrocarbon charging, (3) overpressure and low geothermal gradients reducing cementation and compaction, and (4) late-stage tectonic fracturing that significantly improves permeability. Additionally, dissolution porosity and fracture networks formed during diagenetic and tectonic evolution collectively enhance reservoir potential. The identification of favorable reservoir zones under the sedimentation–diagenesis-tectonics model provides critical insights for future hydrocarbon exploration in ultra-deep clastic sequences.

Keywords: ultra-deep strata; clastic rocks; oil and gas reservoirs; formation mechanisms; hydrocarbon exploration potential

check for updates

Academic Editor: Fabrizio Balsamo

Received: 21 February 2025
Revised: 5 June 2025
Accepted: 13 June 2025
Published: 20 June 2025

Citation: Qi, Y.; Hu, Z.; Wang, J.; Zhang, F.; Wang, X.; Hu, H.; Wang, Q.; Wang, H. The Formation Mechanisms of Ultra-Deep Effective Clastic Reservoir and Oil and Gas Exploration Prospects. *Appl. Sci.* **2025**, *15*, 6984. https://doi.org/10.3390/app15136984

Copyright: © 2025 by the authors. Licensee MDPI, Basel, Switzerland. This article is an open access article distributed under the terms and conditions of the Creative Commons Attribution (CC BY) license (https://creativecommons.org/licenses/by/4.0/).

1. The Lower Limit of Effective Reservoir Burial Depth for Clastic Rocks

In recent years, China's onshore basins have achieved continuous breakthroughs in ultra-deep oil and gas exploration, making the expansion into deeper layers inevitable [1–4]. The Tarim Basin contains 6.77 billion tonnes of petroleum and 9.7 trillion cubic meters (tcm) of natural gas in deep and ultra-deep formations. The Junggar Basin holds 2.84 billion tonnes of petroleum and 2.24 tcm of natural gas. The Sichuan Basin contains 161,300 tonnes of petroleum and 38.11 tcm of natural gas, while the Ordos Basin is estimated to contain 0.1 tcm of natural gas resources. Collectively, these four basins account for over 376 million barrels of oil equivalent (MBOE) in recoverable resources (Table 1). These collective data not only highlight China's growing dominance in global deep-layer hydrocarbon reserves

but also reflect the critical role of tertiary basins in reshaping energy geopolitics. In terms of recoverable crude oil, the Tarim and Junggar Basins are comparable to the Mesopotamian Fordeep Basin in Kuwait (66–72 billion barrels) and Iraq's West Qurna Field (15–21 billion barrels). Regarding natural gas, the Sichuan Basin surpasses Qatar's North and Ras Laffan Fields (over 900 tcf), while the Tarim Basin is comparable to Russia's Urengoy Field (385 tcf). Combined, these four Chinese basins represent the largest known natural gas reserves globally, exceeding Russia's total of 1680 tcf. Traditionally, clastic rocks' primary pores—originally composed of clastic particles, pores, and interstitial materials—gradually diminish during burial. The low solubility of these components limits the formation of secondary pores. As a result, petroleum geologists often define basin-specific lower-depth limits for effective clastic reservoirs [2,5–7]. This concept plays a dual role in exploration, initially guiding efforts toward key strata for breakthroughs but later potentially restricting exploration beyond established limits. However, throughout the exploration history of China's eastern, central, and western basins, the understanding of these depth limits has evolved. As exploration advances, the lower depth limit for effective clastic reservoirs continues to extend downward, undergoing constant reassessment and revision [8–13].

In the early stages, scholars generally defined burial depths greater than 3500–4000 m as deep layers [2,14–16]. Influenced by this understanding, early oil and gas exploration in the eastern Bohai Bay, Songliao, Subei, and central Ordos Basins assumed that the effective reservoir burial depth for clastic rocks was within the same range [1,17,18]. However, intensified exploration in the Tarim, Junggar, and western Sichuan Basins revealed significant structural, geological, and evolutionary differences between the large, superimposed basins with low geothermal gradients in the west and the faulted and down-warped basins in central and eastern China [19–27]. These differences delayed the diagenetic evolution of clastic rocks, shifted exploration targets to deeper layers, and led to the discovery of deeply buried effective reservoirs. Commercial oil and gas discoveries have since been made at ultra-deep realms (>6000 m) [28–31]. Key breakthroughs include Yong 1 (2004) (Yong 1 is a key exploration well in the Junggar Basin, located in the northwest of China) at 5860 m in the Jurassic formation of the central Junggar Basin, Shun-9 (2012) (Shun-9 is an exploration well in the Tarim Basin, a vast basin in southwestern Xinjiang, China) at 5600 m in the Silurian of the Shuntuoguole area in the Tarim Basin, Zheng-10 (2022) (Zheng-10 owned and operated by China Sinopec, a major oil and gas company in China. This well is part of Sinopec's exploration and production activities) at 6700 m in the Triassic Kelamayi Formation and 7600 m in the Upper Wuerhe Formation in the central Junggar Basin, and Cheng-6 (Cheng-6 also owned and operated by China Sinopec) (2022) at 6530 m in the Lower Wuerhe Formation. These discoveries have promoted researchers to redefine the concept of "deep layers" and reassess the lower burial depth limit for effective clastic reservoirs. Recent exploration results confirmed that in the Tarim and Junggar Basins (Table 2), this limit can exceed 8000 m [32–34].

Table 1. Recoverable oil and gas reserves of major global basins.

Country	Basins	Basin Type	Reservoir Age	Lithology	HC Type	Depth	Recoverable Crude Oil ($\times 10^9$ t)	Gas (tcm)	Recoverable Crude Oil [1] (bb)	Gas (tcf)	Total (MBOE)
China	Tarim Basin	Craton	Ordovician	Limestone	Oil, gas	7300	6.77	9.7	49.6	343	109
	Junggar Basin	Craton	Jurassic	Conglomerate sandstone	Oil, gas	5000	2.84	2.24	20.8	79	34
	Sichuan Basin	Craton	Permian–Triassic	Dolomite	Gas	6200–7000	0.0001613	38.11	0.001	1346	232
	Ordos Basin	Craton	Triassic	Sandstone	Gas	5000	-	0.1	-	4	1
Iraq	West Qurna Field	Foreland Basin	Cretaceous	Limestone	Oil, gas	3447	-	-	15–21	-	228,000
Qatar	North and Ras Laffan Field	Passive Margin	Cretaceous	Sandstone	Gas, condensate	3462	-	49.8	-	1760	316,800
Russia	Urengoy Field	Craton	Cretaceous	Sandstone	Gas, condensate	1000–4000	1.2	10.5	8.8	385	68,000
Kuwait	Mesopotamian Foredeep Basin	Foreland Basin	Cretaceous	Dolomite	Oil, gas	3500–5000	-	1.8	66–72	63.6	85,000

[1] Using a conversion of 7.33 barrels per tonne, values may vary based on oil density. Abbreviations: bb = billion barrels; tcm = trillion cubic meters = 1012 m^3; 1 m^3 = 35.3147 cu ft; tcf = trillion cubic feet; BOE = barrel of oil equivalent = 5800 cu ft of gas or 159 L of oil; MBOE = one million BOE.

Table 2. Typical deep clastic rock reservoir characteristics in the four major basins in central and western China. Porosity and permeability are presented as numerical ranges, with average values shown in parentheses.

Basin	Geological Age	Depth (m)	Depositional Environment	Mineral Composition (%)			Grain Size	Sorting	Roundness	Porosity (%)	Permeability (10^{-3} μm^2)
				Quartz	Feldspar	Lithic Fragments					
Tarim	K	5500–8200	Braided River Delta	55	20	25	Medium/Fine Sandstone	Good	Subangular/ Subrounded	5.4–26 (20.4)	
	D	4500–6000	Coastal Sandbar	94	4	2	Medium/Fine Sandstone	Good	Subangular/ Subrounded	5.2–21.8 (18.3)	0.1–2000 (200)
	S	5000–6500	Offshore Sandbar	41	6	53	Fine Sandstone	Good/Moderate	Subangular/ Subrounded	1.4–9.2 (6.3)	0.01–0.84 (0.2)
Junggar	J	3500–6500	Braided River Delta	41	19	40	Medium/Fine Sandstone	Good/Moderate	Subangular/ Subrounded	5–20 (14)	0.1–500 (26)
	T	4600–7200	Alluvial Fan Delta	8	5	87	Sand/Gravel	Moderate/Poor	Subangular/ Subrounded	0.9–21.8 (7.8)	0.01–126 (1.17)
	P	4000–7800	Alluvial Fan Delta	7	11	82	Sand/Gravel	Moderate/Poor	Subangular/ Subrounded	2.6–15 (7.6)	0.01–112 (0.52)
Ordos	T	600–2000	Braided River Delta	49	36	15	Fine Sandstone	Good/Moderate	Subangular/ Subrounded	1.3–19.4 (11.7)	0.01–7.64 (0.56)
	P	2500–3800	Braided River Delta	74	2	24	Medium/Coarse Sandstone	Good/Moderate	Subangular/ Subrounded	1.7–18 (7.6)	0.1–16.4 (0.89)
Sichuan	T	3000–5500	Delta Front	63	24	13	Fine/Medium Sandstone	Good	Subangular	0.5–9.7 (4.1)	0.002–79 (0.61)
	S	3500–6000	Delta Front	87	6	7	Coarse Siltstone	Good/Moderate	Subrounded/ Subangular	0.3–8.67 (2.8)	0.01–4.69 (0.28)
	∈		Shallow Marine Shelf								

With ongoing advancements in oil and gas exploration theory and technology, along with the implementation of Deep Earth Engineering, new breakthroughs in deep-layer oil and gas will continue to reshape researchers' understanding of deep reservoirs. Simultaneously, the burial depth limit and formation mechanisms of effective sedimentary rock reservoirs are being continuously redefined. This paper aims to systematically summarize the development characteristics of effective reservoirs in deep oil-bearing basins in China, clarify their formation mechanisms, and provide reference guidance for future deep-layer sedimentary rock exploration (Figure 1).

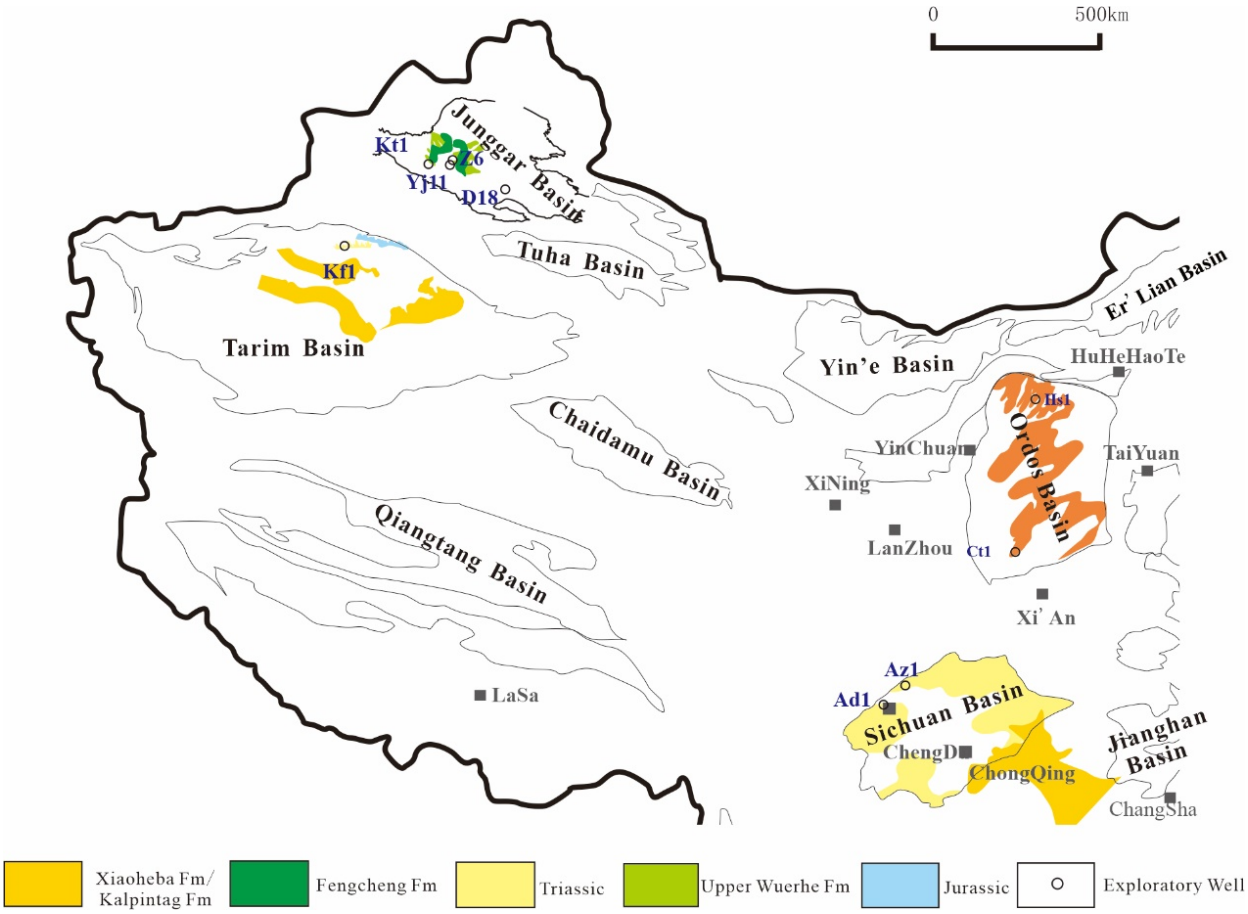


Figure 1. The favorable exploration formations in the central and western regions of China.

2. Formation Mechanisms of Effective Reservoir in Ultra-Deep Clastic Rocks

2.1. Sedimentation Lays the Foundation for Mineral Fabric and Primary Porosity of Reservoirs

The four major basins in central and western China have undergone distinct sedimentation phases: marine sedimentation in the Early Paleozoic, transitional marine–terrestrial sedimentation in the Late Paleozoic, and terrestrial sedimentation since the Mesozoic and Cenozoic. Reservoir properties vary significantly across these basins (Table 1). Overall, the Tarim and Junggar Basins exhibit relatively better reservoir quality, followed by the Ordos Basin, while the Sichuan Basin has the poorest reservoir properties. Reservoirs' characteristics across different basins and sedimentary environments are largely controlled by original sedimentation processes. On a macro scale, sedimentary environments determine the distribution of sedimentary facies, thereby influencing the formation of reservoir sand bodies in oil and gas accumulations [35]. On a micro scale, they affect key factors such as

provenance, grain size, sorting, roundness, and matrix content, which form the material foundation for reservoirs at later stages [36,37].

In marine sedimentary environments, the Devonian Donghetang Formation in the Tarim Basin developed high-energy foreshore facies, depositing pure medium- to fine-grained quartz sandstone with quartz content exceeding 90% (Table 1). Despite long-term deep burial, the grains remain primarily in point-to-line contact, maintaining an average porosity of 18.3% (Figure 2a, Table 1). In contrast, the Silurian Kalpintag Formation in the Shun-9 well area of the Tarim Basin, also comprising coastal sedimentary facies, is characterized by offshore deposits with lithic content generally exceeding 50% (Table 1). As a result, these reservoirs have experienced more intense compaction at similar burial depths. Some exhibit almost no visible pores under a microscope, with plastic lithic fragments compacted into grain pores, leading to relatively poor reservoir quality (Figure 2b, Table 1). Similarly, the Silurian Xiaoheba Formation in the Sichuan Basin primarily developed distal sand bars in a delta-front environment. Coarse clastics are largely absent, and the reservoir consists mainly of siltstone to argillaceous siltstone, resulting in relatively poor reservoir properties (Table 1).

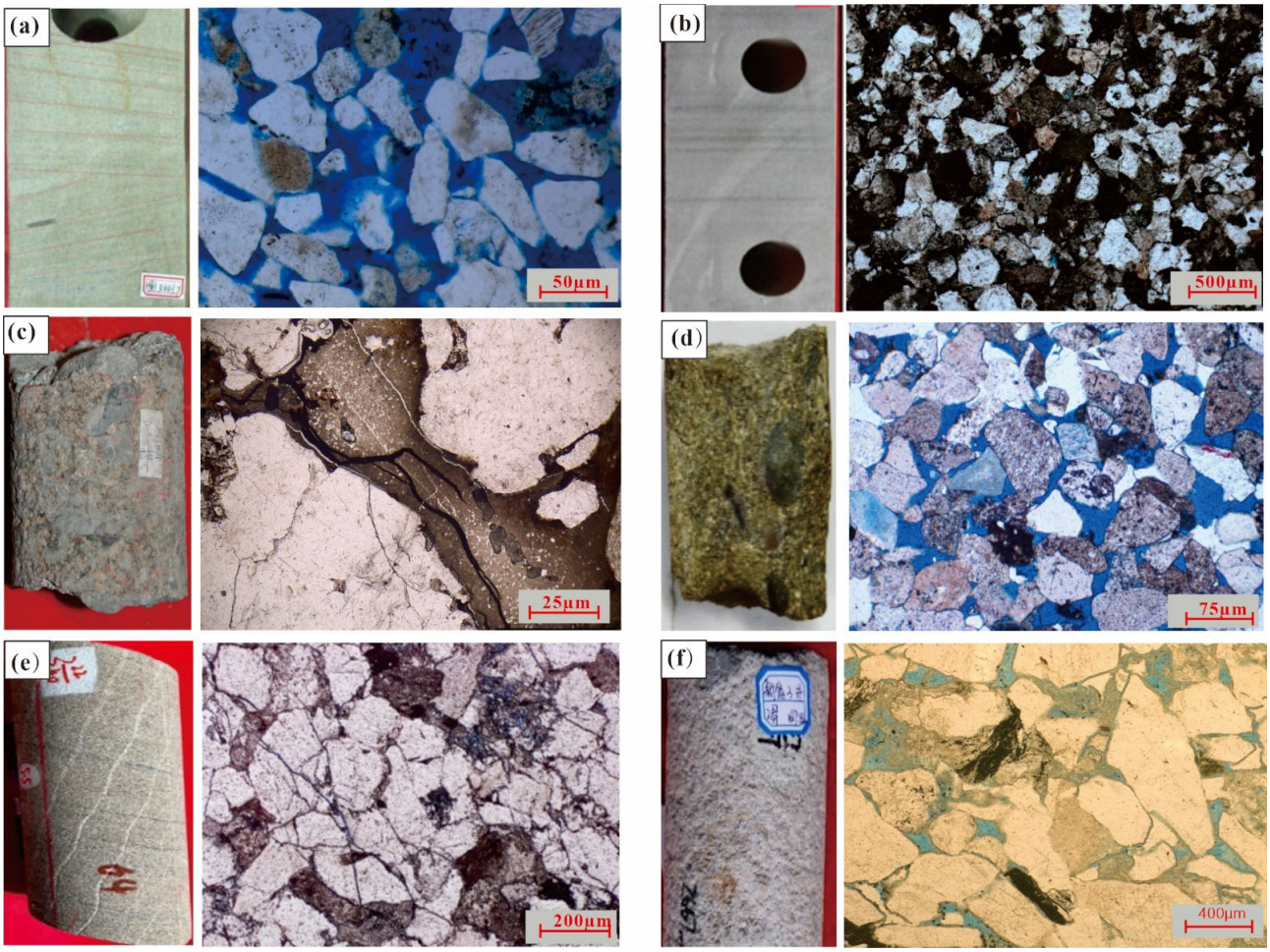


Figure 2. Typical core and thin-section photos of different sedimentary facies zones in the four major basins of central and western regions of China. (**a**) Tarim Basin, D_3d, foreshore bar fine sandstone, Shun-1 well, 5343 m; (**b**) Tarim Basin, S_1k, offshore sand bar fine sandstone, Shun-9 well, 5900 m; (**c**) Junggar Basin, T_1b, delta plain glutenite body, Ma-18 well, 3874 m; (**d**) Junggar Basin, T_2k, delta front fine sandstone, Zheng-10 well, 6701 m; (**e**) Sichuan Basin, T_3x, delta front fine sandstone, Fenggu-110 well, 4624 m; (**f**) Ordos Basin, P_1s, Delta Diversion Channel, Xinfu-3 Well, 2663 m.

Since the Permian–Triassic period [13,24,31], the four major basins in central and western China have progressively transitioned into continental sedimentary environments. In the Junggar basin, thick fan deltas and braided-river delta sandbodies developed during the Triassic. Near the basin margin, in the delta plain close to the provenance area, thick glutenite bodies were deposited. Despite their coarse grain size, sands, gravels, and muds were rapidly mixed and deposited, with tuffaceous material and argillaceous matrix commonly filling the pores (Figure 2c), resulting in poor reservoir properties. Towards the sag area, the sorting and roundness of delta-front sandbodies improve significantly (Figure 2d,f), enhancing reservoir quality and making them prime exploration targets. Recently, Sinopec's Zheng-10 well successfully tested high-yield oil from the delta-front sandbodies of the Triassic Kelamayi Formation, confirming the presence of high-quality reservoirs with 13% porosity at a depth of 6700 m. In contrast, while delta-front channel sandbodies also developed in the contemporaneous Triassic Xujiahe Formation of the Sichuan Basin, stronger compaction and cementation (Figure 2e) have significantly reduced their quality. Currently, porosity in these reservoirs is generally less than 5% (Table 1).

The influence of sedimentary hydrodynamic conditions on reservoir properties is evident not only across different sedimentary microfacies but also within various sections of the same sandbody. Detailed core descriptions and sampling observations from the Silurian (~444–419 Ma) in Shun-9 (Tarim Basin) reveal significant variations in material composition and reservoir quality within a single sandbody (Figure 3a). Generally, at the top of a sandbar, the grain size is coarsest and the plastic grain content is lowest. This zone primarily consists of massive fine-grained sandstones with moderate compaction, and well-developed pores (Figure 3b). In the middle section, fine-grained sandstones with parallel cross-bedding dominate. Compaction is slightly stronger, and primary intergranular pores are only locally preserved (Figure 3c). Towards the bottom, interbedded siltstone and mudstone with wavy bedding appear. Plastic grain content increases, reducing compaction resistance and resulting in strongly compacted lithic sandstones with poor reservoir properties (Figure 3d).

2.2. Multiple Geological Processes Favor the Formation and Preservation of High-Quality Clastic Reservoirs

After deep burial, constructive diagenetic processes play a crucial role in identifying and preserving the reservoir properties of clastic rocks. Scholars have examined the formation mechanisms of deep effective sandstone reservoirs from multiple perspectives [6,14,18,38–41]. Based on previous research, this study critically analyzes the roles of grain coatings, overpressure, geothermal gradients, hydrocarbon charging, dissolution, and fracturing in development and preservation.

2.2.1. Inhibition of Quartz Cement Growth by Grain Coatings

Grain coatings play a crucial role in preventing the widespread nucleation and precipitation of quartz cement on grain surfaces. This mechanism is primarily attributed to the protective barrier formed by grain coatings, which inhibits direct contact between grain surfaces and diagenetic fluids, thereby suppressing cementation. These coatings mainly consist of authigenic clay minerals (predominantly chlorite) and microcrystalline quartz [38,42–44]. Among clay minerals, including illite and mixed layers, authigenic chlorite is the most effective at inhibiting quartz cementation in sandstone. For instance, in the Jurassic Toutunhe Formation of the Junggar Basin, chlorite coatings form continuous rims around quartz grains, significantly reducing quartz overgrowths (Figure 4a). In the Triassic Yanchang Formation of the Ordos Basin, where chlorite coatings are particularly well-developed, their thickness can exceed 10 μm, effectively hindering quartz cementation (Figure 4c). Scanning electron microscopy (SEM) images further confirm that in areas with extensive chlorite development, only minor microcrystalline quartz growth occurs, with

little to no siliceous cementation, thus preserving primary porosity (Figure 4d). Additionally, other authigenic minerals, such as hematite and siderite, can serve similar roles. In the Cretaceous red beds of the Tarim Basin, hematite coatings are common along grain edges, leading to minimal quartz or other cementing minerals observed in thin sections (Figure 4d). More importantly, chlorite coatings contribute to the formation of oil-wet rock surfaces [45]. Under oil-wet conditions, the driving force required for hydrocarbon charging is significantly reduced, effectively enhancing reservoir potential despite otherwise poor reservoir properties [46,47].

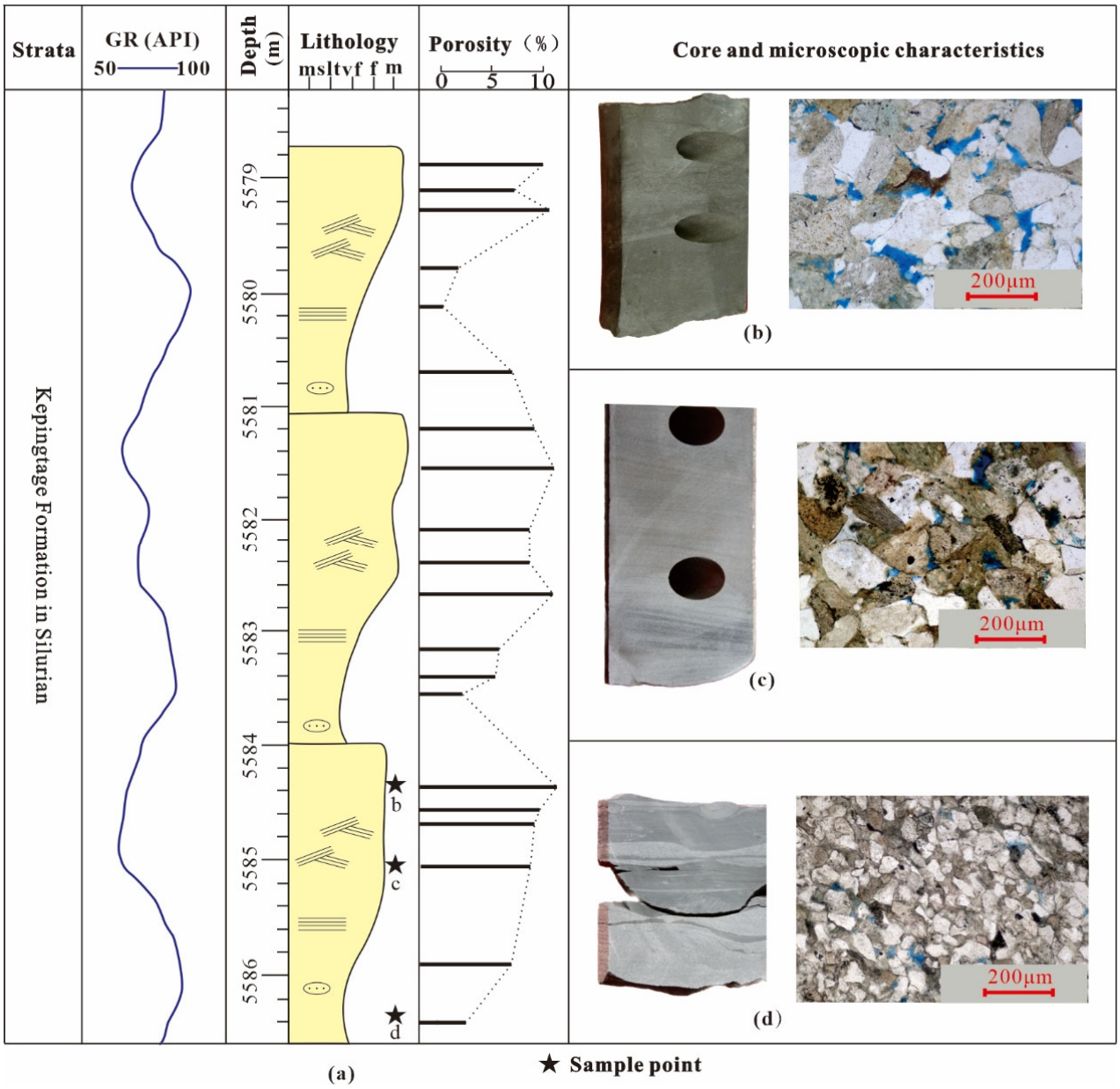


Figure 3. Longitudinal distribution of lithology of Silurian Kepingtag Formation in Tarim Basin and typical microscopic photos. (**a**) Shun-9 well; (**b**) 5584.3 m; (**c**) 5585 m; (**d**) 5586.4 m. ms: mudstone; lt: siltstone; vf: very-fine-grained sandstone; f: fine-grained sandstone; m: medium-grained sandstone.

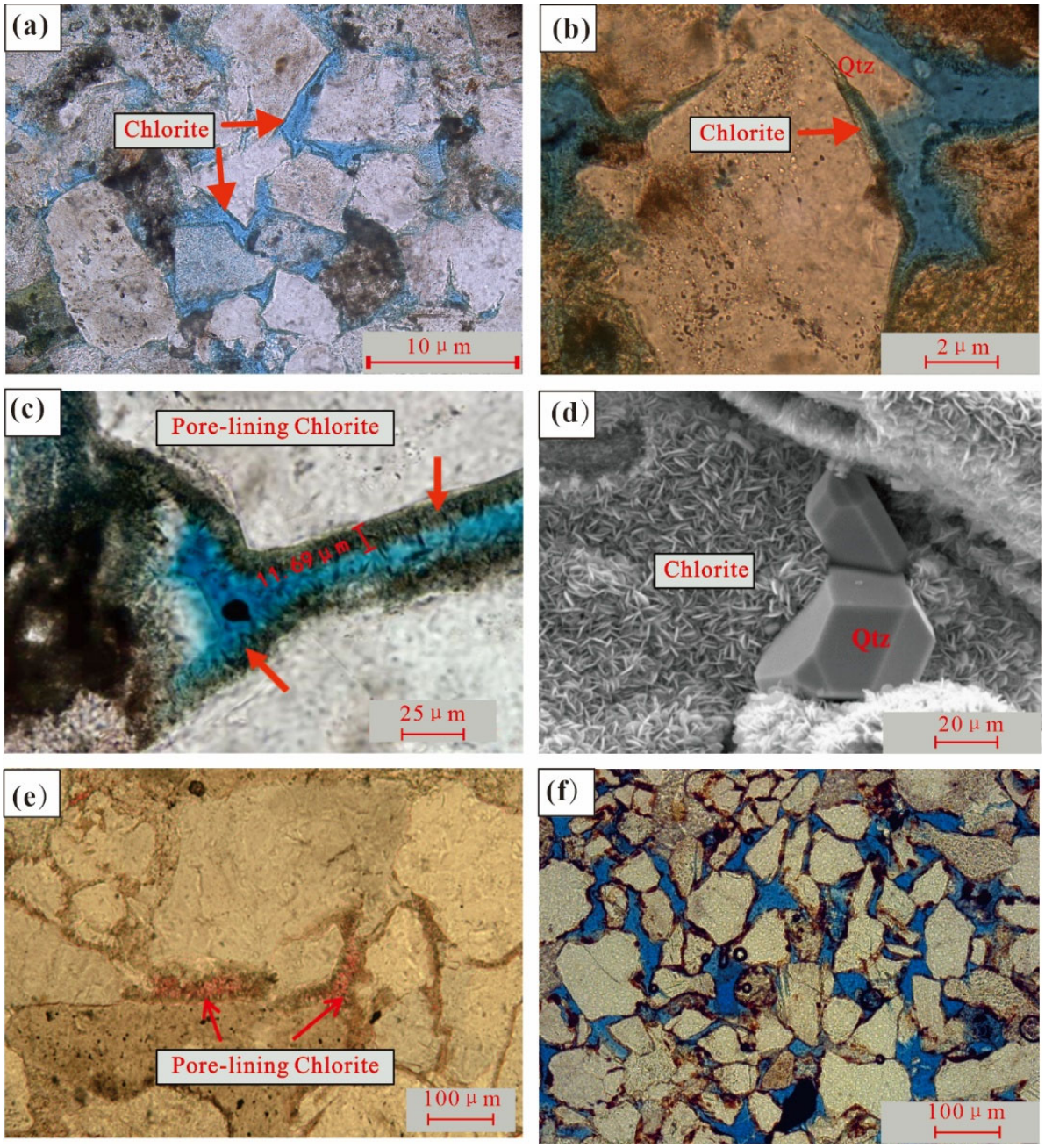


Figure 4. Typical microscopic photos of the effect of grain coating on pore preservation. (**a**) Junggar Basin, J_2t1, Dong-7 well, 4514m; (**b**) Junggar Basin, J_2t1, Dong-2 well, 4429m; (**c**) Ordos Basin, T_3y2, HH45 well, 2350m; (**d**) Ordos Basin, T_3y2, HH45 well, 2350 m; (**e**) Sichuan Basin, T_3x, YL8 wells, 4075.72 m; (**f**) Tarim Basin, K1bs, Xinghuo-5 well, 5600 m.

The effectiveness of grain coatings in inhibiting quartz overgrowth largely depends on the extent of coverage. The greater the surface area of a quartz grain covered by the coating, the more effectively quartz overgrowth is suppressed. Conversely, if coverage is incomplete, quartz overgrowth can still occur [39]. Microscopically, it is often observed that in the same quartz grain, areas not covered by chlorite film can still develop quartz overgrowths due to uneven coating distribution (Figure 4b). Moreover, excessive chlorite content can be detrimental. When chlorite densely fills intergranular spaces, it can significantly reduce or destroy primary intergranular porosity and reservoir permeability [48].

Overall, grain coatings play a crucial role in enhancing the porosity and permeability in deep sandstone reservoirs, which often exhibit anomalously high values. Statistical analyses indicate that higher chlorite content generally correlates with better reservoir properties. However, in cases where cementation is dominated by carbonate, sulfate, or zeolite cements and quartz cementation is relatively weak, the role of grain coatings in preserving primary porosity is diminished. This is particularly evident in sandstones with lower compositional maturity, where quartz cementation is minimal, rendering the impact of grain coatings on porosity preservation negligible.

2.2.2. Inhibitory Effect of Overpressure on Compaction

As the thickness of overlying sediments increases, effective stress on the reservoir rises, enhancing mechanical compaction and reducing porosity. However, the development of pore fluid overpressure can mitigate effective stress and slow the rate of mechanical compaction, thereby preserving primary porosity in sandstone reservoirs. The main mechanisms are as follows: (1) Reduced mechanical compaction: overpressure counteracts effective stress, helping to maintain pore space; (2) Inhibition of intergranular overpressure solution: overpressure limits the dissolution of grain contacts, reducing the supply of silica ions and slowing quartz cementation; (3) Restricted ion exchange: overpressure creates a relatively closed system, significantly decreasing ion exchange with external fluids and effectively slowing cementation [39,49,50].

The preservation of primary pores in reservoirs due to overpressure depends on the mechanical properties of sandstone and the timing of overpressure formation. Sandstone reservoirs with high plastic content have greater pore preservation potential, as compaction primarily controls reservoir quality. Researchers analyzed effective stress and intergranular pore content in core samples from oil fields such as the North Sea and the Gulf of Mexico. Their findings indicate that when effective stress decreases from 80 MPa to 10 MPa, intergranular porosity increases from approximately 15% to 30%, with a maximum of 35%. A similar correlation between porosity and pressure coefficient is observed in the deep layers of major domestic basins, where abnormal high-pressure zones are associated with high-quality reservoir development (Figure 5). For example, in the Zheng-10 well of the Junggar Basin, the high-quality reservoir zone of the Triassic Kelamayi Formation at ~6500 m depth has a pressure coefficient of 1.8 (Figure 5a). In the Kuqa Depression's Cretaceous main production layer, the pressure coefficient exceeds 2.0, with reservoirs exhibiting abnormally high porosity beneath the overpressure zone (Figure 5b). These observations highlight the critical role of overpressure in preserving reservoir porosity [4,51]. Overpressure formation is closely linked to hydrocarbon generation and under-compaction caused by the sealing effects of high-quality gypsum salt caprocks [52,53]. In foreland basins, rapid compaction, tectonic compression, and other geological processes can also contribute to abnormal high-pressure conditions. Therefore, for future deep-basin exploration, identifying formations and zones with efficient source–caprock configurations within hydrocarbon-generating sags will be crucial in locating high-quality reservoirs.

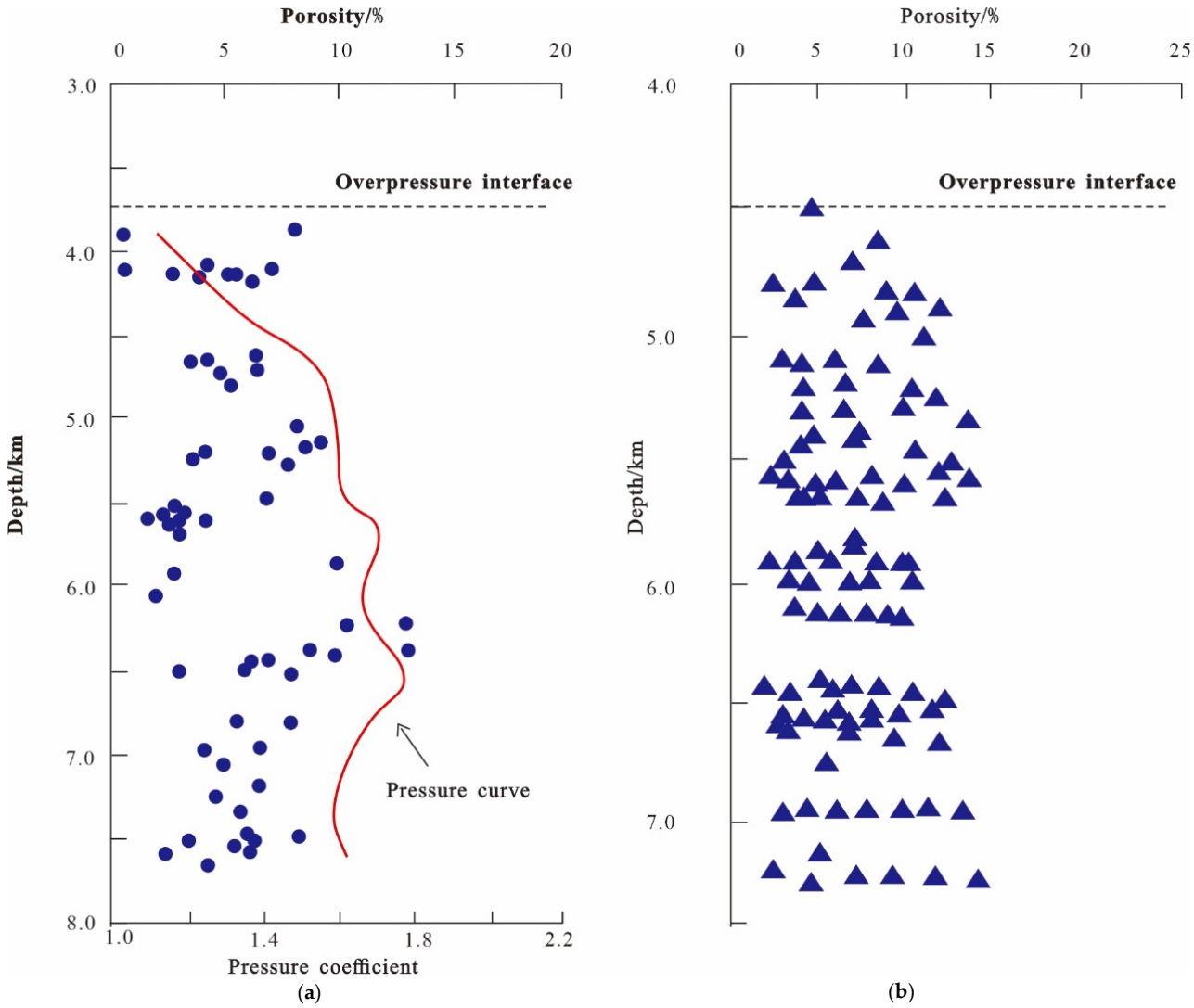


Figure 5. Relationship between overpressure development and porosity of Junggar Basin and Kuqa Depression. (**a**) Zheng-10 well of Junggar Basin; (**b**) Kela-2 well of Kuqa Depression.

2.2.3. Inhibitory Effect of Low Geothermal Field on Diagenetic Evolution

The diagenesis and stages of clastic rock reservoirs are closely linked to the paleogeothermal conditions of the strata. As formation temperature increases, the solubility of authigenic minerals such as quartz and illite decreases in formation water, leading to mineral precipitation [41,54,55]. However, the prolonged lower paleo-heat flow values in China's western basins play a crucial role in delaying diagenesis and preserving reservoir pores. As shown in Figure 6, the Tarim Basin and the Junggar Basin exhibit relatively low paleogeothermal gradients, averaging ~20 °C/km, classifying them as cold basins. At depths of 5000–8000 m, most reservoirs remain in the early sub-stage of the middle diagenetic stage A1 [47], preserving porosity levels of 15–20% (Table 1), primarily characterized by well-developed primary pores. In contrast, the Sichuan Basin and the Ordos Basin have higher geothermal gradients, 30–40 °C/km [11,24]. As a result, their reservoirs have progressed into the late sub-stage of middle diagenetic stage A2 or even middle diagenetic stage B [41]. Consequently, these reservoirs generally exhibit poorer physical properties, with porosity mostly below 10% (Table 1).

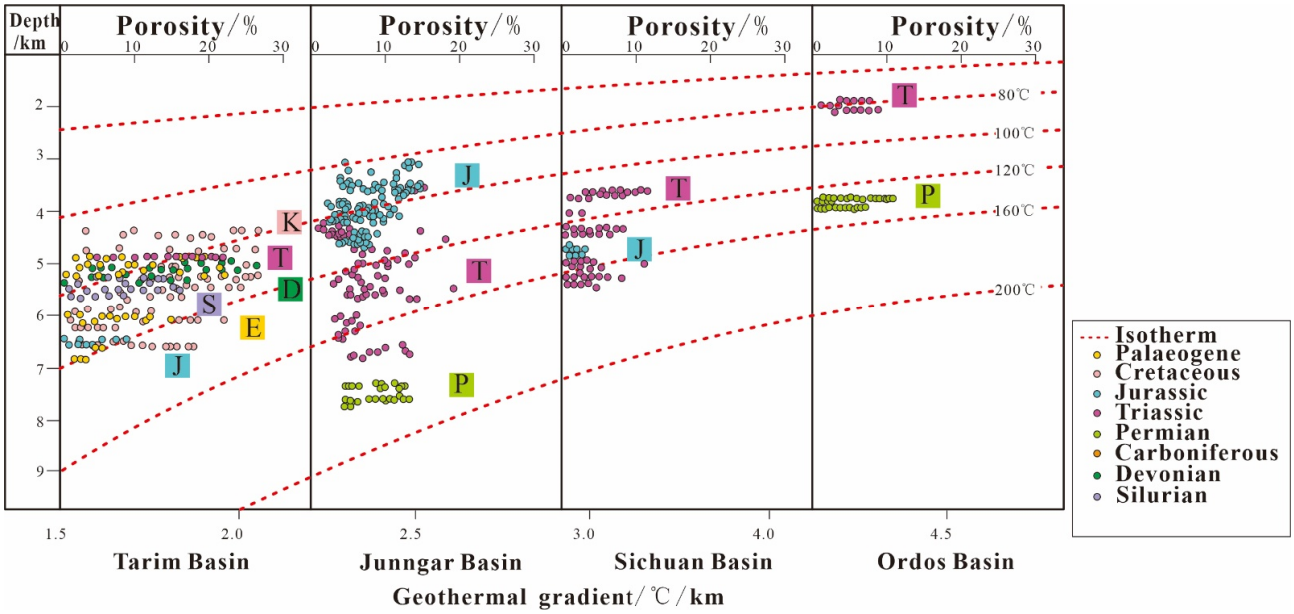


Figure 6. Relationship between geothermal gradients and reservoir properties in the four major basins in the central and western regions of China [11].

The stratigraphic burial processes and rates in different central and western China basins play a crucial role in reservoir pore evolution. In the Kuqa Depression and the southern Junggar Basin piedmont belt, intense compression from Tianshan orogenic uplift during the Himalayan period led to the formation of typical foreland basins. These basins exhibit a burial pattern characterized by slow, shallow burial in the early stage, followed by rapid deep burial in the late stage (Figure 7a,b). For example, in the Cretaceous Bashijiqike Formation, the main productive layer of the Kuqa Depression, subsidence was slow between the Jurassic and Paleogene (130–123 Ma), reaching only about 2000 m [53,56]. However, since the Neogene (23 Ma–present), the strata have rapidly subsided, accumulating thick deposits. Due to the short duration of late-stage rapid deep burial, pore fluids between grains were not fully expelled, limiting compaction. As a result, grain contacts remain predominantly point-line (Figure 4f). In contrast, since the Permian, the Sichuan Basin and Ordos Basin have undergone gradual and continuous subsidence to depths of approximately 5000 m (Figure 7c,d). Consequently, compaction has been more thorough, leading to the complete disappearance of primary pores, with grains exhibiting intergranular fracture (Figure 4e).

2.2.4. Protective Role of Hydrocarbon Charging on Porosity

The role of hydrocarbon charging in preserving porosity has been extensively debated [40,58–60]. Extensive exploration practices and research indicate that early hydrocarbon charging can modify the wettability of reservoir grains, leading to the formation of continuous oil films on grain surfaces. These films inhibit the precipitation of minerals such as quartz, illite, and kaolinite [61–63]. For instance, in the Silurian Kalpintag Formation of the Tarim Basin, significant hydrocarbon charging occurred from the late Caledonian to the late Hercynian periods. Subsequent tectonic uplift and erosion exposed the strata, resulting in crude oil degradation into reservoir bitumen. These early hydrocarbon charges adhered to quartz grain surfaces, altering their wettability and effectively inhibiting later quartz overgrowths. In reservoirs containing bitumen, quartz overgrowths are almost absent, with the combined area percentage of bitumen and residual porosity reaching up to 8.5% (Figure 8a). Conversely, in reservoirs without early hydrocarbon charging, authigenic

minerals like quartz overgrowths are more common, resulting in an average area porosity percentage of only 5.6% (Figure 8b).

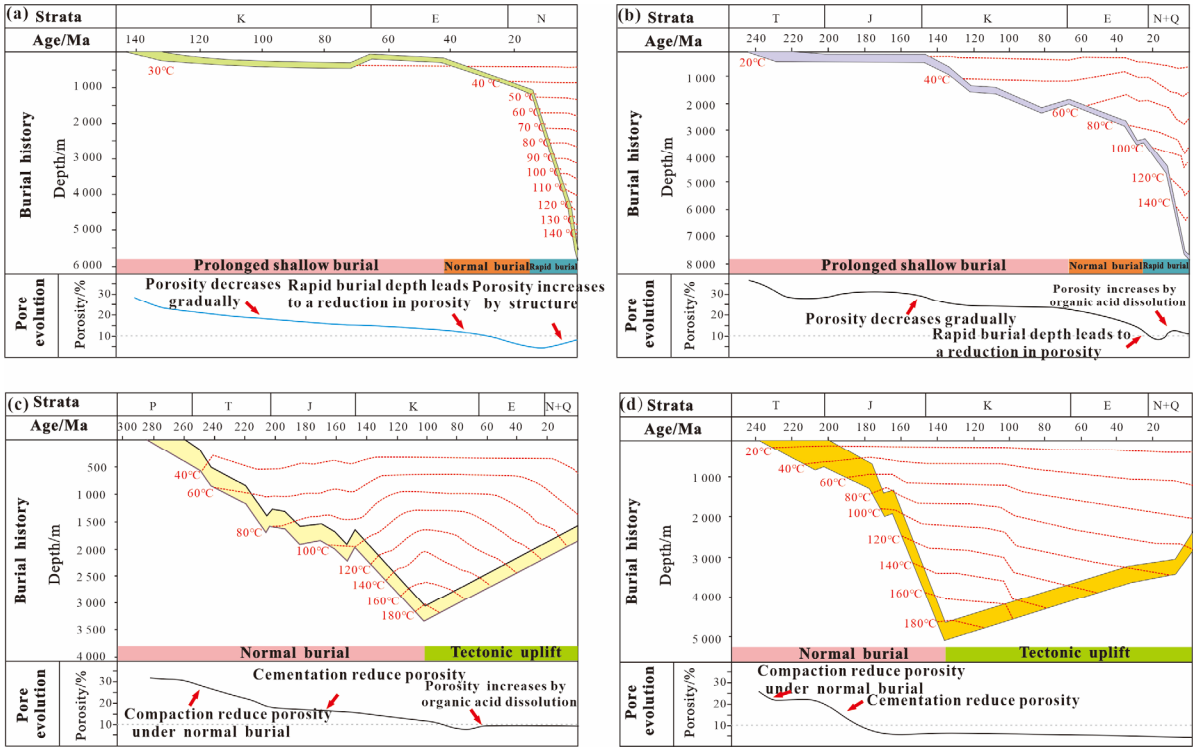


Figure 7. Burial history and pore evolution of key strata in the four major basins in the central and western regions are illustrated [56,57]. (**a**) Triassic strata in the Xinhe area of the southern slope of the Kuqa Depression; (**b**) Cretaceous Qingshuihe Formation in the southern margin of the Junggar Basin; (**c**) Xujiahe Formation in the Puguang area of the Sichuan Basin; (**d**) Permian Shihezi Formation in the Eastern Ordos Basin. These diagrams depict the sedimentary burial processes and their impact on reservoir pore development across the respective basins.

However, the protective effect of hydrocarbon charging on reservoirs largely depends on the wettability of mineral particle surfaces and the timing of oil and gas charging. In many quartz-rich reservoirs, the mixed wettability of quartz surface means some particle surfaces remain hydrophilic [46], making it challenging to form continuous oil films. Consequently, material exchange and mineral precipitation can still occur on mineral surfaces with discontinuous oil films, such as the growth of quartz overgrowth rims (Figure 8c). Therefore, in most cases, hydrocarbon charging can only slow down cementation to some extent, but cannot entirely prevent it.

The timing of hydrocarbon charging significantly influences its effectiveness in inhibiting cementation within reservoirs. In the Kuqa Depression, studies [4] have identified multiple hydrocarbon charging episodes. For instance, research indicates that low-maturity oil entered the reservoirs approximately 5 to 3 million years ago, followed by high-maturity hydrocarbons between 3 and 1.2 million years ago, and a subsequent gas charge from about 1.2 million years ago to the present.

Given that cementation processes typically occur over extended geological periods, these relatively recent hydrocarbon charging events may have had a limited impact on inhibiting cementation within the Kuqa Depression's reservoirs.

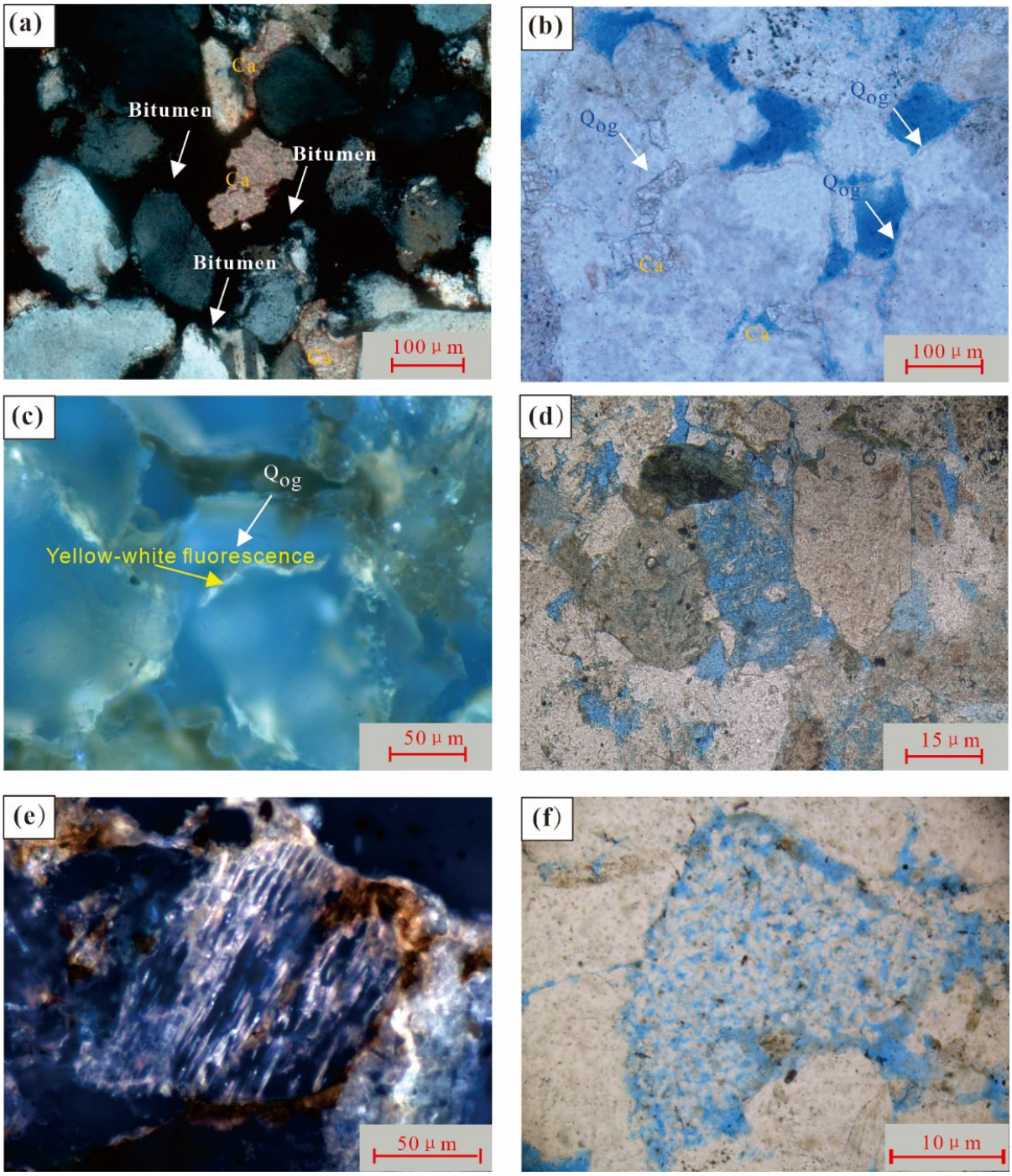


Figure 8. Microscopic characteristics of typical diagenesis in deep reservoirs of the Midwest Basin. (**a**) Silurian, Tarim Basin, Shun-901 well, 5298 m, early hydrocarbon charging effectively inhibited cementation; (**b**) Silurian, Tarim Basin, Shun-9 well, 5397.32 m, quartz overgrowths in bitumen-free reservoir; (**c**) Jurassic, Junggar Basin, Yong-1 well, 5878 m, quartz secondary enlargement outside discontinuous oil film; (**d**) Jurassic, Junggar Basin, Dong-7 well, 5224 m, feldspar dissolution; (**e**) Silurian, Tarim Basin, Shun-902 well, 5518.3 m, two stages of hydrocarbon charging occurred after feldspar dissolution; (**f**) Triassic, Ordos Basin, Honghe-12 well, 2091 m, kaolinite dissolution pores Qog: quartz overgrowth.

2.2.5. Pore-Increasing Effect of Dissolution

The development of dissolution processes in deep-seated reservoirs significantly enhances the reservoir properties of sand bodies. Qualitative petrological observations have led many geologists to conclude that secondary dissolution pores predominate in these

deep-seated sandstone reservoirs [23,63–68]. Microscopic examinations often reveal the dissolution of silico-aluminate minerals, such as feldspar (Figure 8d), which are effective for the migration and accumulation of hydrocarbons. For instance, in the Silurian reservoirs of the Tarim Basin, feldspar grains exhibit pronounced dissolution along joint fractures, with fluorescence imaging indicating that hydrocarbons from two phases migrated along these dissolution pathways (Figure 8e). Beyond the dissolution of detrital minerals, the interaction between diagenetic fluids and authigenic minerals plays a dual role in both preserving and enhancing porosity. Diagenetic early-stage cementation can protect pores from compaction and subsequent acidic or alkaline fluid invasion can dissolve these cements, thereby increasing porosity. Advancements in reactive transport modeling have improved our understanding of subsurface processes by integrating chemical reactions with fluid flow through porous media. These models simulate the spatial and temporal distribution of chemical reactions along flow paths, helping to predict mineral dissolution and precipitation patterns. However, accurately capturing the complex interplay between geochemical reactions and fluid dynamics remains a significant challenge. Early syntaxial calcite cements, while initially occluding pore spaces during shallow burial, can effectively resist compaction. Subsequent diagenetic processes may partially dissolve these cements. In the Silurian reservoirs of the Tarim Basin, evidence shows that quartz grains remain uncontacted, with calcite dissolution residues present in the pores, followed by hydrocarbon migration (Figure 8e). Similarly, the precipitation and later dissolution of kaolinite minerals contribute to pore preservation by releasing additional pore space upon dissolution (Figure 8f).

During burial diagenesis, significant mineral dissolution and the removal of dissolution products by pore-water migration determine the degree of improvement in porosity and permeability. Bjørlykke [69] argued that in a closed geochemical system unaffected by hydrothermal activity, and constrained by material balance, the development of secondary dissolution pores and a net porosity increase are not feasible. Although secondary pores are observable under thin-section microscopy, quantifying the amount of material dissolved and precipitated specifically during a certain diagenetic stage remains highly challenging.

During shallow burial, reservoirs act as open geochemical systems due to meteoric water influence, but in deeper, closed environments, existing geochemical models struggle to predict the formation and distribution of secondary pores, limiting our ability to forecast the dissolution porosity distribution of dissolution pores.

2.3. Structural Fracturing Enhances the Permeability of Clastic Reservoirs

Oil and gas drilling practices have demonstrated that structural fractures are a key factor in improving the flow capacity of deep clastic reservoirs. Nearly all deep and ultra-deep clastic reservoirs in China have been influenced by tectonic activity, making accurate predictions of "sweet spots" with well-developed fractures crucial for achieving high and stable production [66,70–72]. The development of fractures can significantly enhance the matrix permeability of ultra-low permeability or tight reservoirs by providing flow channels for fluid migration.

In recent years, exploration efforts targeting tight sandstone reservoirs using the "fault-fracture body" approach have achieved remarkable success [73–75]. Fractures can even serve as primary storage spaces for hydrocarbons [76,77]. In the Tongjiang–Malubei area of the Sichuan Basin, extensive exploration has shown that fractures can form during early tectonic uplift. Additionally, fractures can develop through processes such as compression, tectonic compaction, and stratigraphic inversion. Various types of fractures can improve the matrix reservoir to differing extents; the reservoir properties of fractured intervals are significantly better than those of non-fractured intervals (Figure 9a).

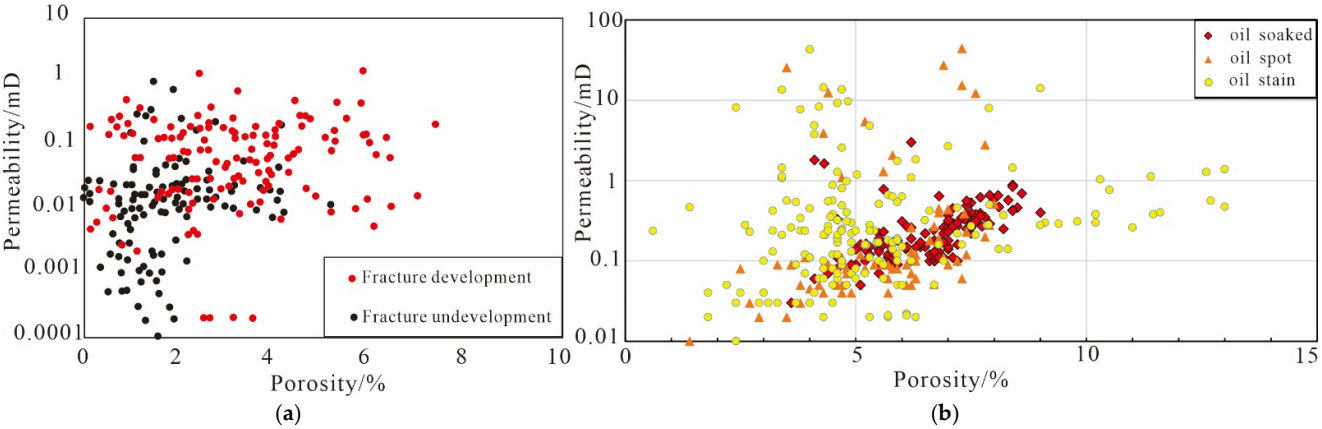


Figure 9. Porosity permeability crossplot for reservoirs in the Sichuan and Tarim Basins. (**a**) Sichuan Basin: Tongjiang Malubei area; (**b**) Tarim Basin: Bozi Dabei area.

In the Shuntuoguole Low Uplift area of the Tarim Basin, fractures effectively connect individual sand bodies in deep sandstone reservoirs, increasing reservoir permeability by 1–3 orders of magnitude (Figure 9b). Furthermore, in most fracture-developed reservoirs, oil traces are visible in the core samples (Figure 9b), indicating that fractures serve as excellent pathways for oil and gas migration. Therefore, overlapping zones of fault-associated fractures, fold-associated fractures, and large-scale high-energy sand bodies represent the "sweet spots" for development.

Fractures can enhance sweet spot grades and even convert non-reservoirs into reservoirs. In the Jurassic–Early Cretaceous phase of the Kuqa Depression, braided river delta sand bodies formed, but their poor matrix porosity has hindered large-scale development. Previous wells drilled by Sinopec and PetroChina failed to achieve industrial oil and gas flow standards. However, the Dibei-5 well and others successfully explored and tested industrial flows using the fault-fracture network without relying on in situ source rocks [33].

3. Exploration Directions for Deep to Ultra-Deep Clastic Rocks

By analyzing hydrocarbon exploration practices and key factors in clastic rock formation and preservation, significant exploration potential remains in deep to ultra-deep strata. The strategy focuses on high-energy sedimentary facies belts, favorable diagenetic zones, reservoir transformation by tectonic fractures, and reservoirs controlled by "trinity" factors. The "trinity" factors—sedimentary facies, diagenesis, and tectonic fractures—are geological controls on reservoir effectiveness, jointly influencing quality, storage capacity, and permeability. A strategic shift from uplift areas to slope zones, closer to the main hydrocarbon source rocks, is a key exploration direction (Figure 1).

3.1. Marine Sedimentary Systems

In the Tarim Basin, the Devonian Donghetang Formation hosts well-developed littoral quartz sandstone. The Hudson oil and gas reservoir was discovered at a structural high. Future exploration will focus on extending towards the sediment source direction from this structural high. In the Silurian Korla Tagh Formation, the Shun-9 reservoir in the Shuntuoguole Low Uplift consists mainly of far-shore sandbar deposits within a high-stand system tract, making reservoir development challenging. Future exploration should focus on deeper deltaic high-energy sedimentary systems in the low-stand system tract. In the Tahe area, multiple wells have penetrated high-quality reservoirs, suggesting that the Tazhong–Shunbei area may share a similar sedimentary background with better reservoir properties. Additionally, NE-trending through-source strike–slip faults can create favorable reservoir development belts controlled by both sedimentary facies and faults. In the

Sichuan Basin, the Silurian–Xiaoheba Formation consists of fine-grained sands, adjacent to Silurian hydrocarbon source rocks. Despite tight reservoirs, high-intensity hydrocarbon charging enables large-scale accumulations. Gas shows have been observed in all sandstone-bearing strata. Recently, Pingqiao-2 in the Fuling area tested a stable industrial gas flow of 25,000 cubic meters, revitalizing tight sandstone exploration. In the Ordos Basin, the Proterozoic Great Wall System features littoral to shallow marine quartz sandstone. Under strong hydrodynamic conditions, high-quality reservoirs with coarse grains, good sorting, and low matrix content have formed. Recent wells indicate exploration potential for self-generating, self-reserving gas reservoirs within the Proterozoic rift trough, making it a promising deep-basin target.

3.2. Continental Depositional System

The intra-source and near-source sedimentary systems in the two major basins north and south of the Tianshan Mountains will be key exploration targets in the coming years. In the central part of the Junggar Basin, the Permian Fengcheng and Lower Wuerhe Formations serve as primary source rocks. Multiple episodes of braided river delta sand deposition have occurred in hydrocarbon-generating depressions such as the Mahu Sag and Pen-1 Well West Sag. These sand bodies are either integrated with or closely adjacent to the source rocks. Repeated hydrocarbon charging and overpressure play a crucial role in reservoir preservation and high-abundance hydrocarbon accumulation. In the Kuche Depression of the Tarim Basin, following the large-scale breakthrough in the Cretaceous Bashijiqike Formation, recent key wells have achieved success in the Triassic and Jurassic source rock formations. Strong tectonic stress compression in the foreland belt has created "fracture-cavity" reservoirs, confirming a source–reservoir integration model and highlighting deeper sag exploration. In the Sichuan Basin, the Triassic Xujiahe Formation contains extensive thick sand bodies, with most discovered gas reservoirs being structural. Future exploration may focus on stratigraphic–lithological reservoirs in slope and sag areas. Despite significant burial depth, tight matrix reservoirs enhanced by fractures and faults remain promising exploration targets.

4. Conclusions

(1) The lower depth limit of effective hydrocarbon reservoirs in clastic rocks is influenced by geological understanding and engineering technology, rather than strict geological boundaries. It evolves with exploration progress and varies across different basins, lithology exploration stages, and technical conditions.

(2) Primary sedimentation determines the mineral composition, grain size, sorting, rounding, and matrix content, shaping the initial pore conditions of clastic rock reservoirs. It also influences diagenesis and pore evolution trends. High-energy sedimentary environments enhance compositional maturity and rigid particle content, providing high-quality reservoirs.

(3) Protective diagenesis processes preserve reservoir pores by inhibiting cementation. Clay mineral films and liquid hydrocarbon charging prevent pore fluids from contacting particle surfaces. A long-lasting low geothermal field can slow diagenesis while overpressure near the major hydrocarbon sources delays reservoir densification, preserving effective clastic rock reservoirs.

(4) In deep reservoirs, high-temperature and high-pressure fluids can induce dissolution, while multi-stage tectonic activity creates complex fractures. These processes enhance porosity and permeability in densified reservoirs, improving sweet spot quality and potentially converting non-reservoirs into reservoirs.

(5) Future exploration should focus on source-rock internal and near-source strata in hydrocarbon-rich depressions. In marine sedimentary systems, the Devonian and Silurian formations near the Manjiaer Depression (Tarim Basin) facilitate vertical hydrocarbon migration, forming large reservoirs controlled by NE-trending strike–slip faults. In the Sichuan Basin, proximity between source and reservoir in the Silurian system is key for tight oil and gas breakthroughs. In continental systems, source–reservoir integration or closely adjacent formations in the P-T (Junggar Basin), the T-J (Tarim Basin), T (Sichuan Basin), and C-P (Ordos Basin) offer prime exploration targets, particularly in the ramp zones of hydrocarbon-rich depressions.

Author Contributions: Conceptualization, Y.Q. and Q.W.; methodology, Z.H.; investigation, Q.W., H.W. and H.H.; writing—original draft preparation, X.W.; writing—review and editing, J.W.; visualization, F.Z. All authors have read and agreed to the published version of the manuscript.

Funding: This research received no external funding.

Institutional Review Board Statement: Not applicable.

Informed Consent Statement: Not applicable.

Data Availability Statement: The raw data supporting the conclusions of this article will be made available by the authors on request.

Acknowledgments: We sincerely appreciate all anonymous reviewers and the handling editor for their constructive comments and suggestions that significantly improved this manuscript.

Conflicts of Interest: Authors Yukai Qi, Zongquan Hu, Jingyi Wang, Fushun Zhang, Hanwen Hu, Qichao Wang and Hanzhou Wang were employed by the company China Petroleum & Chemical Corporation (SINOPEC). Author Xinnan Wang was employed by the company The Third Oil Production Plant of Daqing Oilfield Limited Company. The remaining authors declare that the research was conducted in the absence of any commercial or financial relationships that could be construed as a potential conflict of interest.

References

1. Zhu, G.Y.; Zhang, S.C. Hydrocarbon accumulation conditions and exploration potential of deep reservoirs in China. *Acta Pet. Sin.* **2009**, *30*, 793–802, (In Chinese with English Abstract)
2. Pang, X.Q.; Jia, C.Z.; Wang, W.Y. Petroleum geology features and research developments of hydrocarbon accumulation in deep petroliferous basins. *Pet. Sci.* **2015**, *12*, 1–53. [CrossRef]
3. Guo, H.J.; Si, X.Q.; Yuan, B.; Peng, B.; Ji, D.S.; Chen, X.G. The characteristics and main controlling factors of ultra-deep sandstone reservoir in the middle part of the southern margin of Junggar Basin. *Mar. Orig. Pet. Geol.* **2022**, *27*, 313–324, (In Chinese with English Abstract)
4. Guo, X.S.; Hu, Z.Q.; Li, S.J.; Zheng, L.J.; Zhu, D.Y.; Liu, J.L.; Shen, B.J.; Du, W.; Yu, L.J.; Liu, Z.Q.; et al. Progress and prospect of natural gas exploration and research in deep and ultra-deep strata. *Pet. Sci. Bull.* **2023**, *8*, 461–474, (In Chinese with English Abstract)
5. Ehrenberg, S.N.; Nadeau, P.H. Sandstone vs. carbonate petroleum reservoirs: A global perspective on porosity-depth and porosity-permeability relationships. *AAPG Bull.* **2005**, *89*, 435–445. [CrossRef]
6. Zhong, D.K.; Zhu, X.M.; Wang, H.J. Characteristics and formation mechanism analysis of deep quality clastic rock reservoirs in China. *Sci. Sin. (Terrae)* **2008**, *38*, 11–18, (In Chinese with English Abstract)
7. Wang, B.; Zhang, R.H.; Ren, K.X.; Luo, P.; Liu, C. Prediction of the lower limit of burial depth for effective reservoirs in the Dabei-Kelasu deep structural belt of Kuqa Depression. *Acta Pet. Sin.* **2011**, *32*, 212–218, (In Chinese with English Abstract)
8. Li, J.; She, Y.Q.; Gao, Y.; Yang, G.R.; Li, M.P.; Yang, S. Onshore deep and ultra-deep natural gas exploration fields and potentials in China. *China Pet. Explor.* **2019**, *24*, 403–417, (In Chinese with English Abstract)
9. Zhu, G.Y.; Wang, H.T.; Weng, N.; Yang, H.J.; Zhang, K.; Liao, F.R.; Yuan, N. Geochemistry, origin and accumulation of continental condensate in the ultra-deep-buried Cretaceous sandstone reservoir, Kuqa depression, Tarim Basin, China. *Mar. Pet. Geol.* **2015**, *65*, 103–113. [CrossRef]
10. Xin, Y.; Wang, G.W.; Liu, B.C.; Ai, Y.; Cai, D.Y.; Yang, S.W.; Liu, H.K.; Xie, Y.Q.; Chen, K.J. Pore structure evaluation in ultra-deep tight sandstones using NMR measurements and fractal analysis. *J. Pet. Sci. Eng.* **2022**, *211*, 110–180. [CrossRef]

11. Cao, Y.C.; Yuan, G.H.; Yang, H.J.; Wang, Y.Z.; Liu, K.Y.; Zan, N.M.; Xi, K.L.; Wang, J. Current situation of oil and gas exploration and research progress of the origin of high-quality reservoirs in deep-ultra-deep clastic reservoirs of petroliferous basins. *Acta Pet. Sin.* **2022**, *43*, 112–140, (In Chinese with English Abstract)
12. Deng, Y.; Gao, C.L.; Wang, J.; Liu, M.; Meng, Y.L.; Ren, Y.; Liu, K.; Wang, K. Deep reservoir characteristics and physical property controlling factors of Qigu Formation in western section of southern margin of Junggar Basin. *Mod. Geol.* **2023**, *25*, 1–17, (In Chinese with English Abstract)
13. Wang, J.; Gao, C.L.; Bai, L.; Xiang, B.L.; Liu, J.; Xian, B.Z.; Lian, L.X.; Liu, K. Diagenesis and pore evolution of Cretaceous Qingshuihe Formation reservoir in western section of southern margin of Junggar Basin. *Pet. Geol. Exp.* **2023**, *45*, 632–645, (In Chinese with English Abstract)
14. Sun, L.D.; Zou, C.N.; Zhu, R.K.; Zhang, Y.H.; Zhang, S.C.; Zhang, B.M.; Zhu, G.Y.; Gao, Z.Y. Formation, distribution and potential of deep hydrocarbon resources in China. *Pet. Explor. Dev.* **2013**, *40*, 641–649, (In Chinese with English Abstract) [CrossRef]
15. Bohi, D.R. Technological improvement in petroleum exploration and development. In *Productivity in Natural Resource Industries*; Routledge: London, UK, 2014; pp. 73–108.
16. Scotchman, I.C.; Doré, A.G.; Spencer, A.M. *Petroleum Systems and Results of Exploration on the Atlantic Margins of the UK, Faroes & Ireland: What Have We Learnt? Petroleum Geology Conference Series*; Geological Society of London: London, UK, 2018; Volume 8, pp. 187–197.
17. Wang, C.; Shao, H.M.; Hong, S.X.; Guan, Y.H.; Teng, H.D.; Jia, P.T.; Xue, Y.F. The lower limits of physical properties for deep clastic reservoirs in north Songliao basin and its relationship with microscopic features. *Pet. Geol. Oilfield Dev. Daqing* **2007**, *26*, 18–20+24, (In Chinese with English Abstract)
18. Wang, Y.Z.; Cao, Y.C. Lower Property Limit and Controls on Deep Effective Clastic Reservoirs of Paleogene in Chezhen Depression. *Acta Sedimentol. Sin.* **2010**, *28*, 752–761, (In Chinese with English Abstract)
19. Ma, Y.S.; Cai, X.Y.; Zhao, P.R.; Luo, Y.; Zhang, X.F. Distribution and further exploration of the large-medium sized gas fields in Sichuan Basin. *Acta Pet. Sin.* **2010**, *31*, 347–354, (In Chinese with English Abstract)
20. Song, Y.; Zhao, M.J.; Fang, S.H.; Xie, H.W.; Liu, S.B.; Zhuo, Q.G. Dominant factors of hydrocarbon distribution in the foreland basins, central and western China. *Pet. Explor. Dev.* **2012**, *39*, 285–294. [CrossRef]
21. Huang, H.P.; Zhang, S.C.; Su, J. Palaeozoic oil-source correlation in the Tarim Basin, NW China: A review. *Org. Geochem.* **2016**, *94*, 32–46. [CrossRef]
22. Li, S.; Tang, D.Z.; Pan, Z.J.; Xu, H.; Tao, S.; Liu, Y.F.; Ren, P.F. Geological conditions of deep coalbed methane in the eastern margin of the Ordos Basin, China: Implications for coalbed methane development. *J. Nat. Gas Sci. Eng.* **2018**, *53*, 394–402. [CrossRef]
23. Chen, G.; Hu, Z.Q. Discussion on the model of enrichment and high yield of deep coalbed methane in Yanchuannan area at Southeastern Ordos Basin. *J. China Coal Soc.* **2018**, *43*, 1572–1579, (In Chinese with English Abstract)
24. Guo, X.S.; Hu, D.F.; Huang, R.C.; Wei, Z.H.; Duan, J.B.; Wei, X.F.; Fan, X.J.; Mou, Z.W. Deep and ultra-deep natural gas exploration in the Sichuan Basin: Progress and prospect. *Nat. Gas Ind.* **2020**, *7*, 419–432, (In Chinese with English Abstract) [CrossRef]
25. Hu, S.Y.; Wang, X.J.; Cao, Z.L.; Li, J.Z.; Gong, D.Y.; Xu, Y. Formation conditions and exploration direction of large and medium gas reservoirs in the Junggar Basin, NW China. *Pet. Explor. Dev.* **2020**, *47*, 266–279. [CrossRef]
26. Tian, J.; Wang, Q.H.; Yang, H.J.; Li, Y. Petroleum Exploration History and Enlightenment in Tarim Basin. *Xinjiang Pet. Geol.* **2021**, *42*, 272–282, (In Chinese with English Abstract)
27. Tang, Y.; Song, Y.; He, W.J.; Zhao, L.; Yang, H.B.; Zhao, C.Y.; Zheng, M.L.; Sun, S.; Fei, L.Y. Characteristics of composite hydrocarbon accumulation in a superimposed basin, Junggar Basin. *Oil Gas Geol.* **2022**, *43*, 132–148, (In Chinese with English Abstract)
28. Luo, X.R.; Hu, C.Z.; Xiao, Z.Y.; Zhao, J.; Zhang, B.S.; Yang, W.; Zhao, F.Y.; Lei, Y.H.; Zhang, L.K. Effects of carrier bed heterogeneity on hydrocarbon migration. *Mar. Pet. Geol.* **2015**, *68*, 120–131. [CrossRef]
29. Luo, X.R.; Zhang, L.Q.; Zhang, L.K.; Lei, Y.H.; Cheng, M.; Shi, H.; Cao, B.F. Heterogeneity of clastic carrier bed and hydrocarbon migration and accumulation. *Acta Pet. Sin.* **2020**, *41*, 253–272, (In Chinese with English Abstract)
30. Hu, Z.Q.; Zheng, H.R.; Yin, W.; Liu, C.Y.; Sun, C.X.; Xiao, C.; Wang, F.G.; Li, S.; Chen, C.F. Comparison of diagenetic characteristics and pore evolution in outcrops and cores of tight sandstone reservoirs in the Triassic Yanchang Formation, the Ordos Basin, China. *AAPG Bull.* **2020**, *104*, 2429–2452. [CrossRef]
31. Zhang, X.W.; Pang, X.Q.; Li, C.J.; Yu, J.W.; Wang, W.Y.; Xiao, H.Y.; Li, C.R.; Yu, J.T. Geological characteristics, formation conditions and accumulation model of deep and ultra-deep, high-porosity and high-permeability clastic reservoirs: A case study of Gulf of Mexico Basin. *Acta Pet. Sin.* **2021**, *42*, 466–480, (In Chinese with English Abstract)
32. Shi, C.Q.; Wang, Z.T.; Zhu, W.H.; Jiang, J.; Zhang, H.F.; Zhou, S.Y.; Lou, H.; Zuo, X.J.; Li, G.; Wang, Z. Fracture characteristic and its impact on reservoir quality of ultra-deep reservoir in Dabei region, Kelasu tectonic belt, Kuqa Depression, Tarim Basin. *Nat. Gas Geosci.* **2020**, *31*, 1687–1699, (In Chinese with English Abstract)

33. Wang, K.; Zhang, R.H.; Tang, Y.; Yu, Z.F.; Yang, Z.; Tang, Y.G.; Zhou, L. Structural diagenesis and reservoir prediction of Lower Jurassic Ahe Formation in the northern structural belt of Kuqa depression. *Acta Pet. Sin.* **2022**, *43*, 925–940, (In Chinese with English Abstract)
34. Sun, J.; You, X.C.; Zhang, Q.; Xue, J.J.; Chang, Q.S. Development characteristics and genesis of deep tight conglomerate reservoirs of Mahu area in Junggar Basin. *Nat. Gas Geosci.* **2023**, *34*, 240–252, (In Chinese with English Abstract) [CrossRef]
35. Zou, C.N.; Tao, S.Z.; Zhang, X.X.; He, D.B.; Zhou, C.M.; Gao, X.H. Geologic characteristics, controlling factors and hydrocarbon accumulation mechanisms of China's Large Gas Provinces of low porosity and permeability. *Sci. China (Ser. D Earth Sci.)* **2009**, *52*, 1068–1090. [CrossRef]
36. Qi, Y.K.; Lin, H.X.; Zhang, F.S. The Relationship between Diagenetic Evolution and Hydrocarbon Charge in Deep Tight Reservoirs: A Case Study from Kepingtage Formation of S9 Well Block in Tarim Basin. *Geofluids* **2021**, *2021*, 6665237. [CrossRef]
37. Luo, X.R.; Zhang, L.K.; Zhang, L.Q.; Liu, N.G.; Yan, J.Z.; Lei, Y.H.; Qi, Y.K.; Li, J.; Cheng, M.; Yan, Y.M.; et al. Effectiveness of deep-buried clastic reservoir beds and the evaluation methodology. *J. Northwest Univ. (Nat. Sci. Ed.)* **2022**, *52*, 968–986, (In Chinese with English Abstract)
38. Aase, N.E.; Bjørkum, P.A.; Nadeau, P.H. The effect of grain-coating microquartz on preservation of reservoir porosity. *AAPG Bull.* **1996**, *80*, 1654–1673.
39. Taylor, T.R.; Giles, M.R.; Hathon, L.A.; Diggs, T.N.; Braunsdorf, N.R.; Birbiglia, G.V.; Kittridge, M.G.; Macaulay, C.I.; Espejo, I.S. Sandstone diagenesis and reservoir quality prediction: Models, myths, and reality. *AAPG Bull.* **2010**, *94*, 1093–1132. [CrossRef]
40. Grant, N.T.; Middleton, A.J.; Archer, S. Porosity trends in the Skagerrak Formation, Central Graben, United Kingdom Continental Shelf: The role of compaction and pore pressure history. *AAPG Bull.* **2014**, *98*, 1111–1143. [CrossRef]
41. Cao, Y.C.; Yuan, G.H.; Wang, Y.Z.; Zan, N.M.; Liu, K.Y.; Xi, K.L. Successive formation of secondary pores via feldspar dissolution in deeply buried feldspar-rich clastic reservoirs in typical petroliferous basins and its petroleum geological significance. *Sci. China Earth Sci.* **2022**, *65*, 1673–1703. [CrossRef]
42. Dowey, P.J.; Hodgson, D.M.; Worden, R.H. Pre-requisites, processes, and prediction of chlorite grain coatings in petroleum reservoirs: A review of subsurface examples. *Mar. Pet. Geol.* **2012**, *32*, 63–75. [CrossRef]
43. Pan, R.; Zhu, X.M.; Wang, X.X.; Zhang, J.F. Advancement on formation mechanism of deep effective clastic reservoir. *Lithol. Reserv.* **2014**, *26*, 73–80, (In Chinese with English Abstract)
44. Dutton, S.P.; Hutton, M.E.; Ambrose, W.A.; Childers, A.T.; Loucks, R.G. Preservation of reservoir quality by chlorite coats in deep Tuscaloosa sandstones, central Louisiana, USA. *Gulf Coast Assoc. Geol. Soc. J.* **2018**, *7*, 46–58.
45. Wang, Z.N.; Luo, X.R.; Liu, K.Y.; Fan, Y.C.; Wang, X.Z. Influence of chlorite on wettability in tight sandstone reservoir of Yanchang Formation of Upper Triassic in Ordos Basin. *Sci. Sin. (Terrae)* **2021**, *51*, 1123–1134, (In Chinese with English Abstract)
46. Qi, Y.K.; Luo, X.R.; He, Y.H.; Dang, H.L.; Liu, N.G.; Lei, Y.H.; Zhang, L.K. Experimental studies on oil imbibition in mixed-wetting porous medium. *Chin. J. Geol.* **2015**, *50*, 1208–1217, (In Chinese with English Abstract)
47. Qi, Y.K.; Luo, X.R. Mechanical study of the effect of fractional-wettability on multiphase fluid flow. *Int. J. Multiph. Flow* **2017**, *93*, 205–212. [CrossRef]
48. Zhou, D.S.; Liu, G.X.; Ye, J.; Jia, C.S. Study on the mechanisms for preserving anomalously high porosity in deep buried sandstone reservoirs. *Pet. Geol. Exp.* **2004**, *26*, 40–46, (In Chinese with English Abstract)
49. Walderhaug, O. Modeling quartz cementation and porosity in Middle Jurassic Brent Group sandstones of the Kvitebjorn field, northern North Sea. *AAPG Bull.* **2000**, *84*, 1325–1339. [CrossRef]
50. Lander, R.H.; Bonnell, L.M.; Larese, R.E. Toward more accurate quartz cement models: The importance of euhedral versus noneuhedral growth rates. *AAPG Bull.* **2008**, *92*, 1537–1563. [CrossRef]
51. Duan, W.; Chen, J.D.; Luo, C.F.; Tian, J.Q.; Guo, L.; Lin, J.F. Effects of formation overpressure on diagenesis in the Dongfang block of Yinggehai Basin. *Acta Pet. Sin.* **2013**, *34*, 1049–1059, (In Chinese with English Abstract)
52. Guo, X.W.; Liu, K.Y.; Song, Y.; Zhao, M.J.; Liu, S.B.; Zhuo, Q.G.; Lu, X.S. Influences of hydrocarbon charging and overpressure on reservoir porosity in Kela-2 gas field of the Kuqa Depression, Tarim Basin. *Oil Gas Geol.* **2016**, *37*, 935–943, (In Chinese with English Abstract)
53. Luo, X.R.; Yang, H.J.; Wang, Z.L.; Zhang, L.Q.; Zhang, L.K.; Lei, Y.H.; Zhou, L.; Zhang, B.S.; Yan, Y.M.; Cao, B.F.; et al. Heterogeneity characteristics of deep-ultra-deep clastic rock reservoir and hydrocarbon accumulation model. *Acta Geol. Sin.* **2023**, *97*, 2802–2819, (In Chinese with English Abstract)
54. Jiang, L.Z.; Niu, J.Y.; Zhang, Q.C.; Xu, G.M.; Meng, Y.L.; Xiao, L.H. Major Factors Analysis on Controlling the Formation of Favorable Reservoir in Deep Level of Bohai Bay Basin. *Geol. Rev.* **2009**, *55*, 73–78, (In Chinese with English Abstract)
55. Feng, J.; Gao, Z.Y.; Cui, J.G.; Zhou, C.M. The Exploration Status and Research Advances of Deep and Ultra-Deep Clastic Reservoirs. *Adv. Earth Sci.* **2016**, *31*, 718–736, (In Chinese with English Abstract)
56. Liang, Y.; Liu, X.; Wu, N.; Feng, Y.; Wang, J. Hydrocarbon Accumulation Model Controlled by Overpressure Evolution in the Kelasu Thrust Belt of the Kuqa Depression, NW China. *Lithosphere* **2022**, *2022*, 7352101. [CrossRef]

57. Mejia, P.; Royer, J.J.; Fraboulet, J.G.; Zielińska, A. 4D Geomodeling: A Tool for Exploration—Case of the Kupferschiefer in the Lubin Region, Poland. In *3D, 4D and Predictive Modelling of Major Mineral Belts in Europe*; Weihed, P., Ed.; Springer International Publishing: Cham, Switzerland, 2015; pp. 163–187.
58. Bjørlykke, K. Relationships between depositional environments, burial history and rock properties. Some principal aspects of diagenetic process in sedimentary basins. *Sediment. Geol.* **2014**, *301*, 1–14. [CrossRef]
59. Hermana, M.; Ghosh, D.P.; Sum, C.W. Discriminating lithology and pore fill in hydrocarbon prediction from seismic elastic inversion using absorption attributes. *Lead. Edge* **2017**, *36*, 902–909. [CrossRef]
60. Ramadan, M.A.M.; Abd, E.l.; Hamed, A.G.; Badran, F.; Nooh, A.Z. Relation between hydrocarbon saturation and pore pressure evaluation for the Amal Field area, Gulf of Suez, Egypt. *Egypt. J. Pet.* **2019**, *28*, 1–9. [CrossRef]
61. Yuan, Z.; Li, W.H.; Guo, Y.Q. Effects of Oil Emplacement on Diagenetic Evolution of Sandstone Reservoir in Yanchang Formation, Southeastern Ordos Basin. *Geol. J. China Univ.* **2011**, *17*, 594–604, (In Chinese with English Abstract)
62. Cao, B.F.; Sun, W. Diagenesis of Chang6 Reservoir in Xuecha Block of Wuqi Area. *Nat. Gas Geosci.* **2011**, *22*, 951–960, (In Chinese with English Abstract)
63. Lambert, L.; Durlet, C.; Loreau, J.P.; Marnier, G. Burial dissolution of micrite in Middle East carbonate reservoirs (Jurassic-Cretaceous): Keys for recognition and timing. *Mar. Pet. Geol.* **2006**, *23*, 79–92. [CrossRef]
64. Ehrenberg, S.N.; Walderhaug, O.; Bjørlykke, K. Carbonate porosity creation by mesogenetic dissolution: Reality or illusion. *AAPG Bull.* **2012**, *96*, 217–233. [CrossRef]
65. Baqués, V.; Ukar, E.; Laubach, S.E.; Forstner, S.R.; Fall, A. Fracture, dissolution, and cementation events in Ordovician carbonate reservoirs, Tarim Basin, NW China. *Geofluids* **2020**, *2020*, 9037429. [CrossRef]
66. Rabaev, R.U.; Chibisov, A.V.; Kotenev, A.Y.; Kotenev, M.Y.; Efimov, E.R. Mathematical modelling of carbonate reservoir dissolution and prediction of the controlled hydrochloric acid treatment efficiency. *Sci. Work. NIPI Oil Gas SOCAR* **2021**, *2*, 40–46. [CrossRef]
67. Zhao, X.F.; Zhu, G.Y.; Liu, Q.F.; Zhang, S.C. Main control factors of pore development in deep marine carbonate reservoirs. *Nat. Gas Geosci.* **2007**, *18*, 514–521, (In Chinese with English Abstract)
68. Tan, K.J.; Zhang, F.; Zhao, Y.C.; Pan, J.G.; Yin, L. Characteristics and genetic mechanism of volcanic dissolved pore in northwestern margin of Junggar Basin. *Lithol. Reserv.* **2010**, *22*, 22–25, (In Chinese with English Abstract)
69. Bjørlykke, K.; Jahren, J. Open or closed geochemical system during diagenesis in sedimentary basin: Constraints on mass transfer during diagenesis and the prediction of porosity in sandstone and carbonate reservoirs. *AAPG Bull.* **2012**, *96*, 2193–2214. [CrossRef]
70. Zeng, L.B.; Jiang, J.W.; Yang, Y.L. Fractures in the low porosity and ultra-low permeability glutenite reservoirs: A case study of the late Eocene Hetaoyuan Formation in the Anpeng oilfield, Nanxiang Basin, China. *Mar. Pet. Geol.* **2010**, *27*, 1642–1650. [CrossRef]
71. Guerriero, V.; Mazzoli, S.; Iannace, A.; Vitale, S.; Carravetta, A.; Strauss, C.A. permeability model for naturally fractured carbonate reservoirs. *Mar. Pet. Geol.* **2013**, *40*, 115–134. [CrossRef]
72. Lavenu, A.P.C.; Lamarche, J.; Salardon, R.; Gallois, A.; Marié, L.; Gauthier, B.D.M. Relating background fractures to diagenesis and rock physical properties in a platform-slope transect. Example of the Maiella Mountain (central Italy). *Mar. Pet. Geol.* **2014**, *51*, 2–19. [CrossRef]
73. Wang, J.P.; Zhang, R.H.; Zhao, J.L.; Wang, K.; Wang, B.; Ceng, Q.L.; Liu, C. Characteristics and Evaluation of Fractures in Ultra-deep Tight Sandstone Reservoir: Taking Keshen Gasfield in Tarim Basin, NW China as an Example. *Nat. Gas Geosci.* **2014**, *25*, 1735–1745, (In Chinese with English Abstract)
74. Huang, R.C.; Liu, R.B.; Liu, M.; Cao, H.Y.; Su, S.; Du, H.Q. Characteristics and genesis of fault-fracture reservoirs in the Xujiahe Formation, Tongjiang-Malubei area, northeastern Sichuan Basin. *Oil Gas Geol.* **2021**, *42*, 873–883, (In Chinese with English Abstract)
75. Ma, L.Y.; Qiu, G.Q.; Hu, C.Z.; Xu, S.L.; Chen, C.F.; Li, S. Reservoir Forming Mechanism of the Yanchang Tight Sandstone in Honghe Oilfield, Ordos Basin. *Acta Sedimentol. Sin.* **2022**, *40*, 1762–1773, (In Chinese with English Abstract)
76. Ding, W.l.; Wang, X.h.; Hu, Q.j.; Yin, S.; Cao, X.Y.; Liu, J.J. Progress in Tight Sandstone Reservoir Fractures Research. *Adv. Earth Sci.* **2015**, *30*, 737–750, (In Chinese with English Abstract)
77. Zeng, L.B.; Li, X.Y. Fractures in sandstone reservoirs with ultra-low permeability: A case study of the Upper Triassic Yanchang Formation in the Ordos Basin, China. *AAPG Bull.* **2009**, *93*, 461–477.

Disclaimer/Publisher's Note: The statements, opinions and data contained in all publications are solely those of the individual author(s) and contributor(s) and not of MDPI and/or the editor(s). MDPI and/or the editor(s) disclaim responsibility for any injury to people or property resulting from any ideas, methods, instructions or products referred to in the content.